Dynamics of three anomalous SST events in the Coral Sea

A. Schiller,[1] K. R. Ridgway,[1] C. R. Steinberg,[2] and P. R. Oke[1]

Received 12 December 2008; revised 1 February 2009; accepted 23 February 2009; published 25 March 2009.

[1] Variability of the circulation in the Coral Sea, accompanied by large heat transport anomalies, has the potential to have detrimental impacts on underlying ecosystems, including the Great Barrier Reef. In this study we analyze the dynamics of three events, characterized by extremes in sea-surface temperature, as simulated in an eddy-resolving ocean reanalysis. We show that a cooling in April 1997 results from strong wind anomalies and is supported by vertical and horizontal advective heat losses. A warm event in October 1998 is attributable to a heat gain by horizontal advection. A heat budget of the mixed-layer within a closed box shows that warm anomalies in January 2002 involve a quasi-balance between horizontal advection and vertical entrainment with a large local heat gain through the ocean surface near-shore that apparently caused a coral bleaching event. The dynamics of these extreme events are all quite different, with both local and remote influences.
Citation: Schiller, A., K. R. Ridgway, C. R. Steinberg, and P. R. Oke (2009), Dynamics of three anomalous SST events in the Coral Sea, *Geophys. Res. Lett.*, *36*, L06606, doi:10.1029/2008GL036997.

1. Introduction

[2] The Southwest Pacific is a region of complex ocean circulation. Thermocline waters, carried by various jet-like branches of the westward flowing South Equatorial Current (SEC), split on the Australian eastern boundary to feed the East Australian Current (EAC) and the North Queensland Current (NQC), forming part of a circulation gyre in the Gulf of Papua (Figure 1a). On exit from the Gulf of Papua, the then called Hiri Current (HC) flows into the Solomon Sea and feeds the New Guinea Coastal Current that supplies most of the water of the Equatorial Undercurrent. This circulation, in turn, modulates the ENSO cycle [*Giese et al.*, 2002].

[3] The interannual variability of the circulation and thermodynamics of the Coral Sea are poorly understood due to the lack of appropriate in situ measurements [*Ganachaud et al.*, 2007]. Early studies focused on the climatic mean state and coastal phenomena of the physical oceanography of this region [e.g., *Pickard et al.*, 1977]. Recent coral bleaching events of the Great Barrier Reef (GBR) in early 1998 and 2002 have renewed focus on the adjacent Coral Sea and large-scale circulation pattern [*Steinberg*, 2007; *Weller et al.*, 2008]. Based on an ocean reanalysis [*Schiller et al.*, 2008] provided regional estimates of volume transports for the Coral Sea suggesting large interannual variations in Coral Sea transports. Here, we focus on the temporal variability of thermal properties of the Coral Sea that encompasses the northern half of the GBR.

[4] By using output from a data-assimilating ocean general circulation model this study produces results that are in better agreement with observations than those based on non-assimilating model simulations. The ocean reanalysis is described in detail by *Oke et al.* [2008]. Briefly, the MOM4p0 global hydrodynamic model is used [*Griffies et al.*, 2004], with a resolution of 1/10° in the Asian-Australian region. There are 47 levels in the vertical, with 10 m resolution near the surface. Observations from all available satellite altimeters (ERS, GFO, Topex/Poseidon, Envisat and Jason-1), 57 coastal tide gauges around Australia, plus SST observations from Pathfinder and AMSR-E satellite missions are assimilated into the model. Observations of in situ temperature and salinity from the Argo, TAO and XBT programs are also assimilated into the model. For the region of interest here (142°S to 152°E, 18°S to 11°S) there are typically only 5–10 temperature profiles available each month and virtually no salinity profiles throughout the course of the simulation. The model is forced by 6-hourly atmospheric fields from the 40 year reanalysis ERA-40 of the ECMWF (http://data.ecmwf.int/data/d/era40 daily), including all surface forcing fields, i.e. wind stresses, heat and freshwater fluxes. From September 2003 onwards (end of ERA-40 period) we use the operational ECMWF products as forcing fields.

[5] Section 2 describes the salient features of the mean and seasonal circulation and section 3 discusses three events associated with distinct SST anomalies in the Coral Sea. Section 4 contains a discussion and conclusions.

2. Variability of Circulation

[6] Previous studies [e.g., *Burrage et al.*, 1995] suggested that changes in the intensity and meandering of the SEC in response to climate variability in the Pacific basin could induce significant changes in water masses and currents on the continental shelf and slope of the GBR. The precise location of the bifurcation of the SEC, and the relative intensity of the southern and northern branches, vary both seasonally and interannually. The northern and southern branches form the sources of the NQC in the Coral Sea and the EAC to the south, respectively (Figure 1a). Associated with the quasi-stationary gyre and clockwise circulation around the northern Coral Sea is a relatively small temporal variability in sea level of less than 8 cm for most parts of the region of interest. Using a model simulation, *Kessler and Gourdeau* [2007] argued that, at least for annual variability in the South Pacific, shifts of the bifurcation latitude do not

[1]Centre for Australian Weather and Climate Research, CSIRO Wealth from Oceans National Research Flagship, Hobart, Tasmania, Australia.
[2]Australian Institute of Marine Science, Townsville, Queensland, Australia.

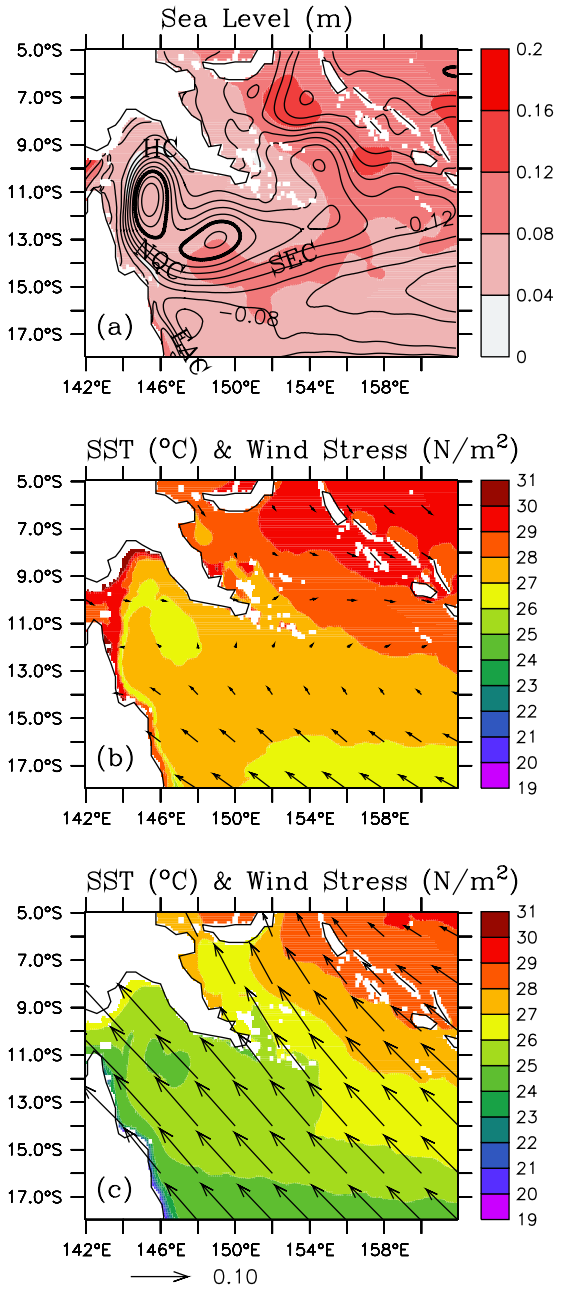

Figure 1. (a) RMS variability of sea level (colour) and mean sea level (contour lines) averaged over period 1992 to 2006. Units are in m. Labels are explained in text. Seasonal SST (°C) for (b) January and (c) July with wind stress vectors superimposed (N/m^2). Reference vectors beneath Figure 1c.

signify corresponding anomalies of transport to the equator, i.e. a migration to the south does not imply stronger northward transports.

[7] The seasonal variability in the strength of the wind stress fields in association with the seasonal solar radiation creates a distinct annual cycle in SST with July SST about 3°C less than the January SST values (Figures 1b and 1c) and a maximum of the annual range in the southern part of the domain. During July the dominant winds are the southeast trades, but during the summer monsoon in January the winds are more variable.

3. Dynamics of Extreme Events

[8] The focus of this study is on the identification of ocean dynamics of SST extremes that affect the Coral Sea and have the potential to disturb the ecosystems along the GBR.

[9] Figure 2a shows time series of the average SST anomaly for the region 142°S to 152°E and 18°S to 11°S in the reanalysis and an equivalent observation-based estimate computed from a SST analysis product with 0.25° resolution [*Reynolds et al.*, 2007]. Both the model- and observation-based time series show a warming trend over the period shown. These trends are around 0.76°C and 0.51°C per decade for the reanalysis and the observations respectively. Based on this short time series, it is not clear whether this trend is evidence of global warming, or part of natural variability. However, we note that a third estimate of the trend in SST anomaly for this period, computed from 15-day composite AVHRR SST observations processed at CSIRO (not shown), shows a similar warming trend of around 0.4°C per decade for this region.

[10] In this section we investigate the ocean dynamics associated with three extreme events in the Coral Sea (Figure 2a). The cases are characterized by cold SST anomalies (case A, April 1997, Figure 2b) and two warm anomalies (case B, October 1998, Figure 2c; and case C, January 2002, Figure 2d). The monthly averaged spatial distributions of these anomalies (Figures 2b–2d) show that virtually the whole Coral Sea is subject to these anomalies, although to a varying degree and with larger amplitude anomalies in the south.

[11] Upper ocean heat content and vertical movement of the thermocline are well represented by the depth of the 20°C isotherm (D20). In the model, the corresponding anomaly of D20 in the Coral Sea is uncorrelated with the SST anomalies. This suggests that there is no simple dynamical relationship, such as a shallowing D20 leading to cooler SST, between those variables as found in other subtropical and tropical areas of the world ocean.

[12] A different conclusion can be drawn from an analysis of the prevailing wind stresses. Figure 2h shows a time series of the anomalies of the magnitude of the wind stresses. It shows a distinct maximum during the peak of the cooling event in April 1997. This maximum is associated with stronger than average southeast trades (Figures 2e and 2i). Conversely, the two warm events happen during, or at the end of, periods where wind stresses are lower than average (Figure 2h). In case B, the wind stresses are weaker than average (Figures 2f and 2j), and Case C shows weak wind stress anomalies of typically less than 0.02 N/m^2 (Figures 2g and 2k). As shown in the subsequent text associated changes in latent flux and surface net heat flux and their impact on the heat budget are limited except for one special situation.

[13] To quantify the dynamic balances that lead to these anomalous cooling and warming events we calculate the heat budget for the box defined in Figure 2b. Horizontal temperature fluxes are calculated across the lateral box boundaries and across the time-dependent 26°C isotherm

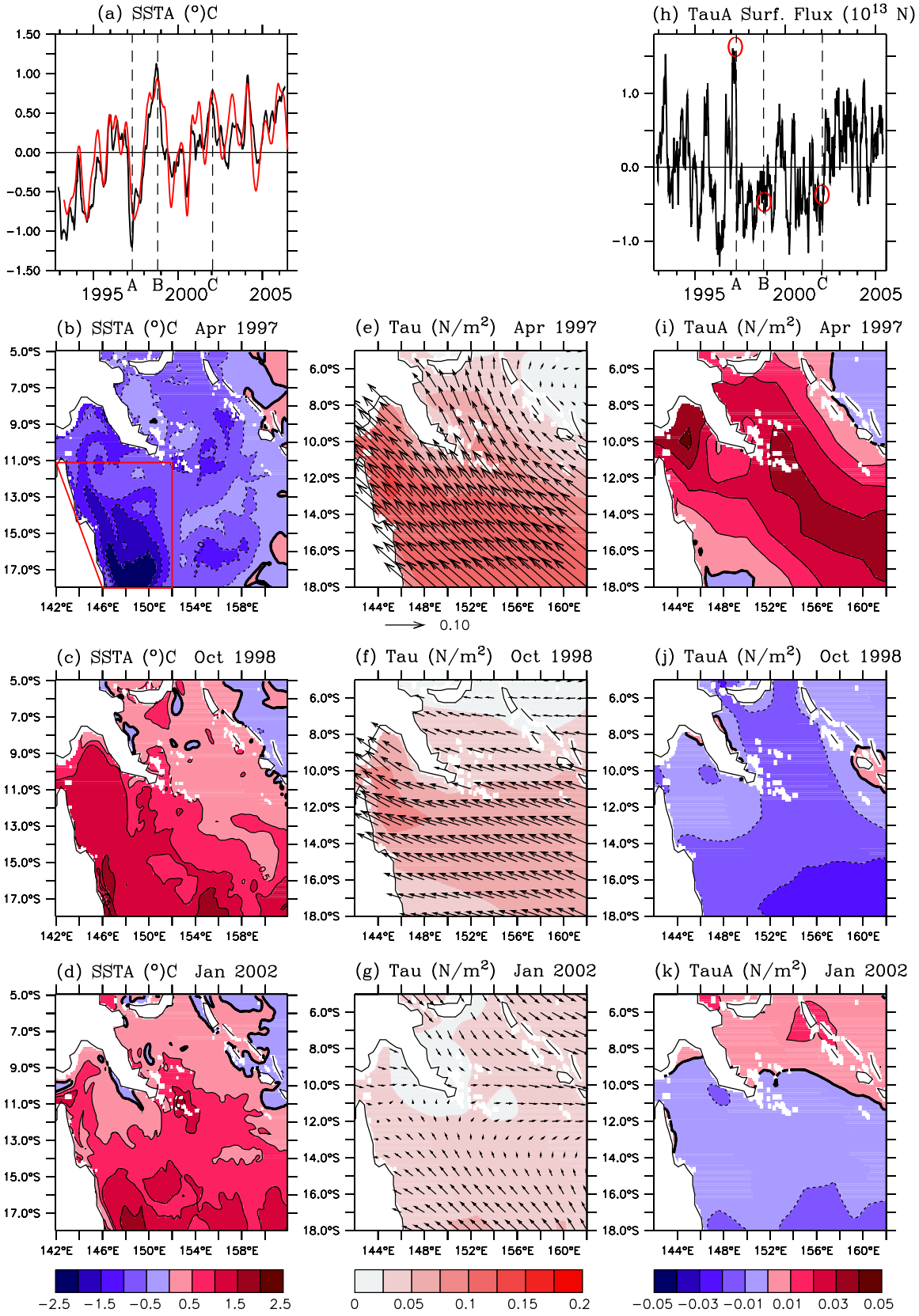

Figure 2. (a) SST anomalies for region marked in Figure 2b for reanalysis (black line) and observations (red line). (b)–(d) SST anomalies (°C) and (i)–(k) anomalies of wind-stress magnitude (N/m^2) for April 1997, October 1998 and January 2002. (e)–(g): wind stress (vectors) and magnitude (colour). Reference vector under Figure 2e. (h) Area-integrated anomalies of wind stress magnitude (10^{13}N) for region marked in Figure 2b. A 3-monthly running-mean filter has been applied to Figures 2a and 2h.

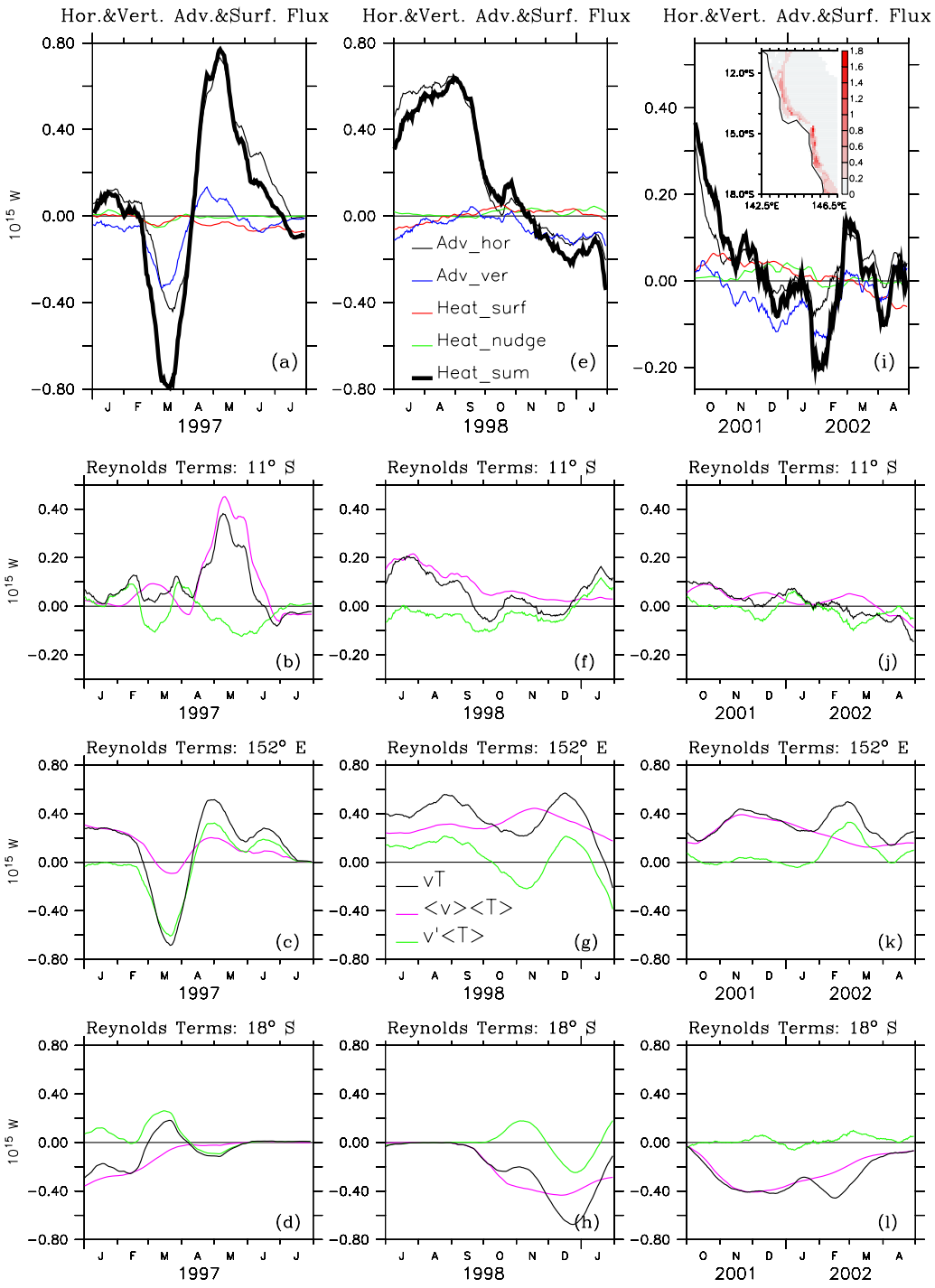

Figure 3. (a, e, i) Temperature budget above depth of 26°C isotherm for box shown in Figure 2b for three different periods: horizontal, vertical advection, surface net heat flux, source term from data assimilation and sum of terms (thick line). Labels shown in Figure 3e. (b, f, j) Reynolds decomposition of horizontal advection across 11°S. Labels shown in Figure 3g are explained in text. (c, g, k) Same as for Figures 3b, 3f, and 3j but for 152°E. (d, h, l) same as above but for 18°S. Units are in 10^{15} W. Positive values denote heat gain of box. A monthly running-mean filter has been applied to all data. Inlay in Figure 3i: January 2002 temperature difference (°C) between z = 5m and z = 25m for coastline of box shown in Figure 2b.

which was chosen as a proxy for the lower boundary of the surface mixed-layer. The surface net heat flux is the ECMWF product. Contributions from horizontal and vertical diffusion are not discussed here as they are orders of magnitudes smaller than the advective terms. We also show the contribution from an additional forcing term that is associated with the data assimilation. This term results from sequentially nudging the model to a three-dimensional

analysis field [*Oke et al.*, 2008] and is integrated over the whole region from the depth of the 26°C isotherm to the surface. This term is quite small (typically 10% or less of all contributions to the heat balance) but shown here for completeness.

[14] The results of this analysis (Figures 3a, 3e, and 3i) show the contributions for periods plus/minus three months of the respective extreme events. The thick line denotes the sum of the surface net heat flux, horizontal/vertical advection and nudging term. The cold anomaly in Case A is the sum of a significant heat loss of all components in the two months preceding the negative SST anomalies in April 1997 (Figure 2b). This event is associated with the passing of tropical cyclone ''Justin'' through the Coral Sea that advected and entrained comparably cold water into the upper Coral Sea. Notably, the strong cooling is balanced by an equally large heat gain in the subsequent months that is largely provided by horizontal advection. Case B (Figure 2c) shows the dominant impact of horizontal (positive) temperature advection on the heat balance in the Coral Sea in the months prior to October 1998. After this time the positive anomalies are slowly eroded by heat losses through vertical and horizontal advection. In contrast to the distinct dynamics of cases A and B the reasons leading to the warm anomalies in case C (Figure 2d) are less obvious. Here, horizontal and vertical temperature advection into the box is almost zero or even slightly negative in the months prior to January 2002. However, the warming in October 2001 is of interest as it ''preconditions'' the area for the eventual bleaching event on the GBR in January 2002. Furthermore, there is a notable small, but steady heat gain through the ocean's surface for the three months preceding January 2002 [*Weller et al.*, 2008].

[15] To gain further insight into the contributions from the horizontal circulation to the SST anomalies a Reynolds decomposition is performed. Horizontal temperature fluxes are decomposed into seasonal mean (< >) and anomalies from the seasonal cycle ($'$) (the latter representing ocean interannual and intraseasonal (eddy) variability). Integration of these temperature fluxes along a section and over depth yields the associated advective ''heat transport'' across this section:

$$\int\int vTdxdz = \int\int \rho c_p(\langle v\rangle\langle T\rangle + \langle v\rangle T' + v'\langle T\rangle + v'T')dxdz \quad (1)$$

v denotes the velocity component normal to a section and integrations are performed along a section. All components of this decomposition are integrated over depth from the daily mean depth of the 26°C isotherm to the surface. ρ denotes the density of sea water and c_p is the specific heat capacity at constant pressure. We refrain from a further separation of the deviations into interannual and intraseasonal components due to a seamless spectrum (i.e. the life cycle of eddies can extend into the interannual spectrum).

[16] We note that in all cases investigated here the terms $\langle v\rangle T'$ and $v'T'$ are an order of magnitude smaller than typical values for the other terms, so we omit them from the plots for clarity. The fact that T' is small means that in general the mean temperature advection associated with the mean velocity and the interannual and eddy velocity anomalies should be the key contributors to temperature fluxes. This is confirmed by inspection of Figures 3b–3d which shows the Reynolds fluxes for case A through the northern (11°S), eastern (152°E) and southern (18°S) lateral boundaries of the box shown in Figure 2b. The key contributor to the negative SST anomalies in case A is a heat loss through the eastern boundary through the $v'\langle T\rangle$ term, i.e. interannual and eddy-flux of momentum associated with the mean temperature field (Figure 3c). Beyond April 1997, the cold anomalies are eroded by (mainly) $\langle v\rangle\langle T\rangle$ seasonal fluxes through the northern boundary and heat gains from $v'\langle T\rangle$ and $\langle v\rangle\langle T\rangle$ across the eastern boundary. Zero values in Figure 3d correspond to a period when the 26°C isotherm outcrops at the surface.

[17] Case B (Figures 3f–3h) shows that most of the heating that leads to anomalously high SST in October 1998 occurs through combined advection of $\langle v\rangle\langle T\rangle$ and $v'\langle T\rangle$ into the domain, the former across the northern and eastern boundaries and the latter across the eastern boundary (≈20–30% of total advective heat gain). In case C (Figures 3j–3l) heat advection across the northern boundary is almost zero and the seasonal contributions $\langle v\rangle\langle T\rangle$ cancel each other across the eastern and southern boundaries (i.e. seasonal temperature advection from east to south with negligible storage in the interior).

[18] The coral bleaching event on the GBR in early 2002 (case C) is the most severe in recent history [*Steinberg*, 2007]. To understand the somewhat intriguing causes of this event we note that Figure 3i represents an area-average for the domain shown in Figure 2b and Figures 3j–3l are the corresponding temperature fluxes across the three sections. The inlay in Figure 3i shows the monthly-mean temperature difference within the box between the surface level of the model (z = 5m) and z = 25m. A coastal strip with enhanced positive anomalies is visible right along the GBR with a temperature difference $\Delta T_{(z=5m-z=25m)}$ that locally exceeds 1.8°C. For comparison: this positive temperature difference along the GBR is largest for all individual seasons during the reanalysis period and with local extrema typically less than 0.5°C. These results suggest that in the absence of significant advective contributions and in the presence of weak winds the coral bleaching event in early 2002 was largely driven by persistent net heat gain through the surface (Figure 3i). Consistent with these findings the mixed-layer during this anomalously warm period was very shallow along the coastal strip of the box (approximately 20m, not shown).

[19] Further investigation of the warm event in January 2002 reveals that the moderate but prolonged heat gain through surface fluxes in an area along the GBR and averaged over a period from October 2001 to January 2002 is ≈70 W/m^2. Although horizontal advection achieves some cooling (−37 W/m^2) the surface fluxes dominate and cause a gradual increase in SST which peaks in January 2002 (SST > 30°C), ultimately leading to the associated coral bleaching event.

4. Discussion and Conclusions

[20] This study uses an eddy-resolving ocean reanalysis to infer interannual variability and dynamical drivers of SST anomalies in the Coral Sea.

[21] Preconditions for coral bleaching events on the GBR are known to be simultaneous factors of low winds, weak currents, no clouds (i.e. strong solar insolation) and no swell (M. Heron, personal communication, 2008). Swell-induced mixing is not simulated by this model. However, all other factors have been identified and quantified for the three cases presented in this study. Interannual and eddy-induced velocity times seasonal temperature advection ($v' \langle T \rangle$) into the Coral Sea becomes important during extreme events (e.g., Figure 3c). Otherwise, it is mostly the combined effect of advection of seasonal temperature by seasonal velocities ($\langle v \rangle \langle T \rangle$) that determines the SST budget in this region. Latent and surface net heat fluxes are less important in modulating extreme events unless the advective contributions cancel each other (e.g. case C).

[22] Despite these successful simulations the model used here has some shortcomings. The model does not include explicit tidal forcing. By contrast, the circulation in the Coral Sea, and particularly along the coasts, are affected by tides. Consequently, results shown here such as the warming event in early 2002 (case C) along the GBR and associated vertical temperature profiles are likely to be modulated by tides. The tidal influence can be in the form of enhanced mixing that can alleviate the surface heat build up if a cooler sub-surface layer exists, redistributing the heat throughout the water column. One source of cold bottom water are intrusions across the shelf break that are either tidally driven or from other mesoscale phenomena lifting the thermocline up over the shelf. Conversely, the persistent stratification can result in a more stable two-layer system trapping heat near the surface. If the tides are too weak to mix bottom waters toward the surface then the stability of the water column is strengthened by any solar heating especially when winds are low. This allows for a shallower stable surface layer with a potential to amplify rather than erode any near surface temperature gain through surface heat fluxes.

[23] Another limitation of the model is that it involves a sequential nudging of the model state towards an observation-based analysis as part of the data assimilation scheme. This complicates the analysis of the model by effectively adding an artificial forcing term to each model equation. Through analysis of the relevant terms in the regional heat budget (e.g., Figure 3), we show that the dynamical mechanisms identified as causes of extreme events in the Coral Sea dominate the nudging term and therefore help us understand the causes of the events considered here.

[24] Combined observational and modeling studies such as the ongoing international Southwest Pacific Circulation and Climate Experiment (SPICE) [*Ganachaud et al.*, 2007] and the GBR Ocean Observing System as part of the Australian Government's Integrated Marine Observing System are designed to further unravel the dynamics of regional and basin-scale climate variability of this ecologically sensitive and unique region.

[25] **Acknowledgments.** This publication is a contribution to the project Bluelink—Ocean Forecasting Australia and to the Australian Government's Marine and Tropical Sciences Research Facility.

References

Burrage, D. M., R. D. Hughes, L. Bode, and D. B. McWilliams (1995), Dynamic features and transports of the Coral Seas, in *Recent Advances in Marine Science and Technology*, edited by O. Bellwood, H. Choat, and N. Saxena, pp. 95–105, PACON Int., Honolulu, Hawaii.

Ganachaud, A., et al. (2007), Southwest Pacific Ocean Circulation and Climate Experiment (SPICE). Part I. Scientific background, *CLIVAR Publ. Ser. 111*, 37 pp., Int. CLIVAR Proj. Off., Southampton, U. K.

Giese, B. S., S. C. Urizar, and N. S. Fuckar (2002), Southern Hemisphere origins of the 1976 climate shift, *Geophys. Res. Lett.*, *29*(2), 1014, doi:10.1029/2001GL013268.

Griffies, S. M., R. C. Pacanowski, and A. Rosati (2004), A technical guide to MOM4, *GFDL Ocean Group Tech. Rep. 5*, 371 pp., NOAA Geophys. Fluid Dyn. Lab., Princeton, N. J.

Kessler, W. S., and L. Gourdeau (2007), The annual cycle of circulation of the southwest subtropical Pacific, analyzed in an ocean GCM, *J. Phys. Oceanogr.*, *37*, 1510–1627, doi:10.1175/JPO3046.1.

Oke, P. R., G. B. Brassington, D. A. Griffin, and A. Schiller (2008), The Bluelink Ocean Data Assimilation System (BODAS), *Ocean Modell.*, *21*, 46–70, doi:10.1016/j.ocemod.2007.11.002.

Pickard, G. L., J. R. Donguy, C. Henin, and F. Rougerie (1977), *A Review of Physical Oceanography of the Great Barrier Reef*, *Monogr. Ser.*, vol. 2, 134 pp., Aust. Inst. of Mar. Sci., Townsville, Queensl.

Reynolds, R. W., T. M. Smith, C. Liu, D. B. Chelton, K. S. Casey, and M. G. Schlax (2007), Daily high-resolution-blended analyses of sea surface temperature, *J. Clim.*, *20*, 5473–5496.

Schiller, A., P. Oke, G. Brassington, M. Entel, R. Fiedler, D. Griffin, and J. Mansbridge (2008), Eddy-resolving ocean circulation in the Asian-Australian region inferred from an ocean reanalysis effort, *Progr. Oceanogr.*, *76*, 334–365, doi:10.1016/j.pocean.2008.01.003.

Steinberg, C. (2007), Impacts of climate change on the physical oceanography of the Great Barrier Reef, in *Climate Change and the Great Barrier Reef*, edited by J. E. Johnson and P. A. Marshall, pp. 51–74, Great Barrier Reef Mar. Park Auth., Townsville, Queensl., Australia.

Weller, E., M. Nunez, G. Meyers, and I. Masiri (2008), A climatology of ocean-atmosphere heat flux estimates over the Great Barrier Reef and Coral Sea: Implications for recent mass coral bleaching events, *J. Clim.*, *21*, 3853–3871.

P. R. Oke, K. R. Ridgway, and A. Schiller, Center for Australian Weather and Climate Research, CSIRO Marine and Atmospheric Research, Castray Esplanade, GPO Box 1538, Hobart, Tas 7001, Australia. (andreas.schiller@csiro.au)

C. R. Steinberg, Australian Institute of Marine Science, Townsville, Qld 4810, Australia.